Am J Cancer Res 2023;13(9):4073-4086
www.ajcr.us /ISSN:2156-6976/ajcr0150302

Original Article

BMP signaling inhibition overcomes chemoresistance of prostate cancer

Chen Xie[1], Zhijun Wang[2], Yong Ba[3], Jose Aguilar[1], Austin Kyan[1], Li Zhong[4], Jijun Hao[1]

[1]College of Veterinary Medicine, Western University of Health Sciences, Pomona, CA 91766, USA; [2]Department of Clinical Pharmacy Practice, School of Pharmacy & Pharmaceutical Sciences, University of California, Irvine, CA 92697, USA; [3]Department of Chemistry and Biochemistry, California State University, Los Angeles, CA 90032, USA; [4]College of Osteopathic Medicine of the Pacific, Western University of Health Sciences, Pomona, CA 91766, USA

Received March 22, 2023; Accepted August 17, 2023; Epub September 15, 2023; Published September 30, 2023

Abstract: Chemoresistance is a major therapeutic challenge to prostate cancer and its underlying molecular mechanism is poorly understood. Previously, it has been suggested that bone morphogenetic protein (BMP) signaling is down-regulated during the prostate cancer progression from the early androgen-sensitive stage to the metastatic castration-resistant stage. However, no literature reports are available for BMP signaling in more advanced-chemoresistant prostate cancer. In this study, we found the expression levels of the BMP type I receptor members, Activin-like kinase-2 (ALK2) and Activin-like kinase-3 (ALK3), were significantly higher in the chemoresistant prostate cancer cells than those in the chemosensitive prostate cancer cells. In addition, the phospho-Smad1/5/9 proteins, the pivotal intracellular effectors of the BMP signaling, were notably elevated in the chemoresistant prostate cancer cells over the chemosensitive prostate cancer cells, indicating that BMP signaling is highly activated in the chemoresistant prostate cancer cells. We also found that BMP signaling inhibition with either DMH1 or the knockdown of ALK2/ALK3 sensitized chemoresistant prostate cancer cells to the chemotherapy drug docetaxel in a dose-dependent manner. Our further study indicates that DMH1 suppressed the migration and invasion of chemoresistant prostate cancer cells *in vitro*, and attenuated chemoresistant prostate tumor growth in the mouse xenograft model *in vivo*. In addition, we showed that DMH1 disrupted the sphere formation in DU145-TxR and PC3-TxR cells, and suppressed the expression of marker genes of the cancer stem cells (CSCs). In conclusion, our study demonstrates that BMP signaling is associated with prostate cancer chemoresistance and BMP signaling inhibition effectively overcomes the cancer chemoresistance potentially through the disruption of CSCs' stemness.

Keywords: Chemoresistance, prostate cancer, DMH1, BMP signaling, cancer stem cells, xenograft

Introduction

Prostate cancer is the second most common cancer and a leading cause of cancer death among men worldwide [1]. In the early stage, prostate cancer is generally androgen-dependent and androgen-deprivation therapy (ADT) can effectively inhibit the growth of prostate cancer [2-4]. Nevertheless, prostate cancer may eventually stop responding to ADT and becomes androgen independent, also known as castration-resistant prostate cancer (CRPC). Docetaxel (Taxotere) is one of the main chemotherapy drugs to treat metastatic CRPC. However, patients treated with docetaxel generally develop chemoresistance, a major therapeutic problem for prostate cancer treatment [5]. Currently, molecular mechanisms for prostate cancer chemoresistance are poorly understood and effective therapies are not available.

BMP signaling is mediated through transmembrane serine/threonine kinases, BMP type I and type II receptors [6]. Extracellular BMP ligands promote the formation of a heteromeric complex consisting of two type II kinase receptors and two type I kinase receptors. This complex-ligand aggregate enables the BMP type II receptors to phosphorylate the type I receptors, resulting in further phosphorylation of the intracellular Smad 1/5/9 (phospho-Smad1/5/9) proteins. The phospho-Smad1/5/9 proteins then form a complex with Smad4 and translocate into the nucleus to regulate the expression

of transcriptional genes such as Id1, Id2, and Id3 [6]. During prostate cancer progression from the early androgen-dependent stage to the metastatic CRPC stage, the expression of BMP2 and BMP4 ligands becomes lower or absent, and BMP type I and type II receptors are frequently deregulated in metastatic prostate cancer [7-11]. In addition, Smad4, a critical downstream protein to transduce extracellular BMP signals to the nucleus for target gene transcription, is often lost in CRPC as well [12]. In summary, the literature indicates that BMP signaling is down-regulated from the early androgen-sensitive stage to the metastatic CRPC stage. However, to date, no studies have been reported on the BMP signaling in the more advanced- chemoresistant prostate cancer. In this study, we examined the expression of the four BMP type I receptors and BMP activation in both the chemosensitive and chemoresistant prostate cancer cells. In addition, we investigated the effects of DMH1, a BMP signaling inhibitor specifically targeting BMP type I receptor, on the chemoresistance of prostate cancer cells as well as DMH1 efficacy for the chemoresistant prostate cancer in a mouse xenograft model [13].

Materials and methods

Cell culture and reagents

The human CRPC prostate cancer cell lines DU145 and PC-3 were obtained from American Type Culture Collection (ATCC, Manassas, VA, USA), and the docetaxel-resistant cell lines (DU145-TxR and PC3-TxR) were a gift from Professor Moses S. S. Chow (College of Pharmacy, Western University of Health Sciences, Pomona, CA, USA). They were cultured in RPMI 1640 supplemented with 10% FBS (Gibco) and 1% penicillin/streptomycin (GenClone®) in an atmosphere of 5% CO_2 at 37°C. Docetaxel was purchased from Sigma-Aldrich Co. (St Louis, MO, USA) and docetaxel injection solution (20 mg/mL) used for *in vivo* study was purchased from Covetrus (Portland, ME, USA). DMH1 (4-[6-[4-(1-Methylethoxy)phenyl]pyrazolo[1,5-a] pyrimidin-3-yl]-quinoline) (CAS No.: 1206711-16-1; Molecular weight: 380.44) was purchased from Selleck Chemicals LLC (Houston, TX, USA). Hydrogen Chloride (4 mol/L in 1,4-dioxane) (Molecular weight: 36.46, CAS RN®: 7647-01-0) was purchase from TCL. 2-Hydroxypropyl-β-cyclodextrin (2-HP-β-CD, CAS No.: 128446-35-5; Average molecular weight: 1,460) was purchased from Millipore Sigma.

Protonated DMH1 chloride for in vivo study

Commercial DMH1 was modified into protonated DMH1 chloride to improve the solubility of DMH1 for the *in vivo* animal study. Briefly, the DMH1 powder from Selleck Chemicals LLC was first dissolved in dioxane under vortex, and then 3-4 times of the HCl 1,4-dioxane solution was added to the solution, which was vortexed for a further 30 min. The solution was frozen using liquid nitrogen and then lyophilized under a high vacuum until the solid powder was obtained, which was further incorporated into 2-HP-β-CD to form an inclusion complex. To collect the hazardous HCl gas, a vacuum line was installed with a liquid nitrogen cold trap to condense the HCL gas and the 1,4-dioxane solvent. A calcium carbonate trap was followed to absorb the remaining HCl gas in the vacuum line.

Cell viability assay

The cell viability was measured based on a colorimetric MTT assay using CellTiter 96® AQueous One Solution Cell Proliferation Assay (Promega, Madison, WI, USA). Briefly, cells were seeded in a 96-well plate and incubated at 37°C in a 5% CO_2 incubator overnight followed by different treatments for 72 hrs. Then 20 μL of CellTiter 96® AQueous One Solution Reagent was added to each well of the 96-well plate containing the samples in 100 μL of cell culture medium for 1 hr. The absorbance was read on a POLARstar spectrophotometer (BMG Labtech, Cary, NC, USA) at 490 nm. The results were expressed as the percentage of treated cells compared to untreated control using the equation: $Viable\% = \frac{Absorbance(Test)}{Absorbance(Control)} \times 100$. All the readings were normalized to the control. The control cell viability was designated as 100%. The experiments were performed in triplicate for each treatment group.

Cell scratch-wound assay

PC3, DU145, PC3-TxR and DU145-TxR cells were seeded in 35 mm dishes and cultured to confluence. The wounds were scratched by a pipette tip in the center of the culture. The cells were washed and treated with DMSO, docetax-

el (1 nM), DMH1 (3 μM) or the combination of docetaxel (1 nM) and DMH1 (3 μM), respectively. Photographs were taken when wounds were created and after 24-hrs' incubation by using phase-contrast microscopy. The distance of each scratch closure was quantitatively evaluated using software ImageJ. A minimum of three randomly chosen areas were measured. The distance of cell migration to the wound area was calculated as following: $\textit{Migration rate}(\%) = \frac{(D0 - Dn)}{D0} \times 100$, where D0 represents the initial scratch width, Dn represents the width at 24 hrs.

Modified Boyden chamber invasion assay

Cell invasion was assessed by 24-Multiwell Insert chambers (8 μm pore size, GenClone®) according to the manufacturer's instructions. The cell culture inserts were coated with Matrigel (BD Biosciences, San Jose, CA, USA). The cells were seeded followed by 72-hrs' incubation with or without different treatments.

Cells that had not moved to the lower wells were removed from the upper surface of the filters by scraping them with cotton swabs. The cells that penetrated through the Matrigel and were adherent to the bottom of the membrane were fixed in 4% paraformaldehyde (PFA) for 10 min followed by staining in 0.2% crystal violet for 5 min. Then the invasion cells were counted under a microscope manually. Mean values for three randomly selected fields were obtained for each well. Experiments were performed in duplicate, and the mean values were presented.

Western blotting

Cells were lysed with RIPA buffer (Sigma-Aldrich, St Louis, MO, USA) supplemented with protein inhibitors (complete ULTRA Tablets, Roche) and phosphatase inhibitors (PhosSTOP, Sigma-Aldrich, St Louis, MO, USA). Samples were denatured by incubating at 95°C for 5 min in the sample buffer. After being separated by SDS-PAGE gels, the proteins were transferred to a PDVF membrane (Millipore, Burlington, MA, USA). The membrane was blocked with Odyssey Blocking solution (Li-Cor Biosciences, Lincoln, NE, USA) for 1 hr at room temperature, followed by primary antibody incubation at 4°C overnight. Primary antibodies used were mouse anti-beta actin (Cell Signaling Tech, Danvers, MA, USA), rabbit anti-p-Smad1/5/9 (#13820, Cell Signaling Tech, Danvers, MA, USA), mouse anti-Smad 1/5 (ab75273, Abcam, Waltham, MA, USA), rabbit anti-ALK2 (SAB1306388, Sigma-Aldrich, St Louis, MO, USA) and rabbit anti-ALK3 (ab174815, Abcam, Waltham, MA, USA). The proteins were detected by an Odyssey system (Li-Cor bioscience, Lincoln, NE, USA) followed by the secondary antibodies including IRDye 680-conjugated goat anti-rabbit IgG (Li-Cor Bioscience, Lincoln, NE, USA) and IRDye 800CWconjugated goat anti-mouse IgG (Li-Cor Bioscience, Lincoln, NE, USA).

Real-time PCR

Total RNA was extracted using an RNeasy Mini kit (Qiagen, Hilden, Germany) following the manufacturer's protocol. The first strand cDNAs were synthesized using the High-capacity cDNA Reverse Transcription kit (Thermo Fisher Scientific, Waltham, MA) according to the manufacturer's instructions. Quantitative real-time PCR was performed using Fast Syber Green (2×) Master Mix (Thermo Fisher Scientific, Waltham, MA) in triplicate on Bio-Rad CFX connected Real-Time PCR system. The human glyceraldehyde-3-phosphate dehydrogenase (GAPDH) gene was used as an internal control. The primer sets used in this study are shown in Supplementary Table 1.

Transfection

For the knockdown experiments, DU145-TxR and PC3-TxR cells were seeded in 96-well plates in the growth medium RPMI1640/10% FBS without antibiotics. The cells were transfected with Fugene HD transfection reagent (Promega, Madison, WI, USA) following the manufacturer's instructions using ALK2 Human siRNA oligo Duplex (SR300056, OriGene, Rockville, MD, USA) or ALK3 human siRNA oligo Duplex (SR300454, OriGene, Rockville, MD, USA) at a concentration of 20 nM, respectively. Negative control siRNA duplex (SR30004, OriGene, Rockville, MD, USA) was also used as the control.

Tumor xenograft and drug administration

The animal experimental protocol was approved by the Western University of Health Sciences Institutional Animal Care and Use Committees (IACUC) which follows the Guide for the Care

and Use of Laboratory Animals of the National Institutes of Health. A total of 40 NSG mice (NOD.Cg-Prkdcscid Il2rgtm1Wjl/SzJ) from the Jackson laboratory (#005557) were used in this study. PC3-TXR cells were cultured in the cell culture medium, harvested, resuspended in serum-free RPMI1640 and diluted by Matrigel (BD Biosciences, San Jose, CA, USA) and PBS (1:1). Approximately 1×10^6 cells were then subcutaneously implanted into the right flank region of mice. When the xenograft tumors reached about 100 mm^3 (*tumor volume* = $\frac{(Width2\times Length)}{2}$), where Width is the tumor measurement at the widest point, and Length is the tumor dimension at the longest point), the mice were randomly divided into four groups and treatment was started as the Day 0: a) the vehicle control group (saline i.v. injection/once per week, 12.5% HP-β-CD, i.p. injection/every other day), b) docetaxel treatment group (20 mg/kg docetaxel i.v. injection/once per week), c) DMH1 treatment group (5 mg/kg protonated DMH1 chloride dissolved in 12.5% HP-β-CD i.p. injection/every other day), d) docetaxel plus protonated DMH1 chloride (20 mg/kg docetaxel i.v. injection/once per week, 5 mg/kg protonated DMH1 chloride dissolved in 12.5% HP-β-CD i.p. injection/every other day). The docetaxel solution was administered once a week for two weeks. Tumor volumes were measured twice a week. The tumor tissues were dissected and weighed at the end of the study. Parts of the tumor tissues were frozen at 80°C and the rests were fixed immediately in 10% neutral buffered formalin.

Immunofluorescence staining

The tumor tissue was fixed in 10% Neutral buffered formalin and then placed into 30% sucrose solutions at room temperature. The tumor tissues were quickly frozen in OCT compound (Fisher HealthCare) in liquid nitrogen. The frozen OCT block was then sectioned (10 μm thick) using a cryostat (Leica, Model CM 1950, Germany). For the immunocytochemistry staining, the slices were washed with PBS three times and blocked with 5% normal goat serum (Cell Signaling Tech, Danvers, MA, USA) with 0.3% Triton X-100 in PBS for 1 hr at room temperature. The slices were incubated overnight with primary antibody Ki67 (#9449, Cell Signaling Tech, Danvers, MA, USA) at 4°C in a humidity chamber. In the next day, the slices were washed three times with PBS, and then incubated for 2 h at room temperature with fluorescent secondary antibody Alexa Fluor® 488 conjugate (#4408, Cell signaling Tech, Danvers, MA, USA). The slices were then washed three times with PBS. Finally, the slices were coverslipped with Prolong® antifade reagent with DAPI (#8961, Cell Signaling Tech, Danvers, MA, USA). Immunofluorescence images were taken with Zeiss LSM 880 confocal microscope. Data and images were analyzed with Image J software and analyzed via Student's t-test. $P<0.05$ was considered statistically significant.

Sphere formation assay

Cells were plated at 1000 cells/mL on a low-attached 6-well-plate for suspension culture. Cells were grown in serum-free Prostate Epithelial Cell Growth Basal Medium (Lonza Walkersville, MD, USA) supplemented with 4 μg/mL insulin (Sigma-Aldrich, St Louis, MO, USA), B27 (Thermo Fisher Scientific, Waltham, MA, USA), 20 ng/mL basic fibroblast growth factor (bFGF; Sigma-Aldrich), 20 ng/mL epidermal growth factor (EGF; Sigma-Aldrich, St Louis, MO, USA) for 14 days. The sphere-forming capacity was assessed by the number of colonies and the sphere size larger than 50 μm diameter was calculated. The Images were taken using an EVOS FL microscope (Thermo Fisher Scientific, Waltham, MA, USA).

Statistical analysis

All values are expressed as means ± SEM unless specified in the figures. The results of different groups were compared using a one-way analysis of variance (ANOVA), followed by the post-hoc Bonferroni test for multiple comparisons. Comparison of the means between two groups was conducted using Student's t-test with GraphPad Prism 8.3.1 (GraphPad, San Diego, CA, USA), and the results were considered statistically significant if the *p*-value is less than 0.05.

Results

ALK2 and ALK3 expression levels are enhanced in the chemoresistant prostate cancer cells

The BMP type I receptor is indispensable for BMP signaling regulation, and it consists of four members (ALK1, ALK2, ALK3 and ALK6), each of which can mediate the BMP signaling. We examined the mRNA expression of all four BMP type I receptor members by RT-PCR in both

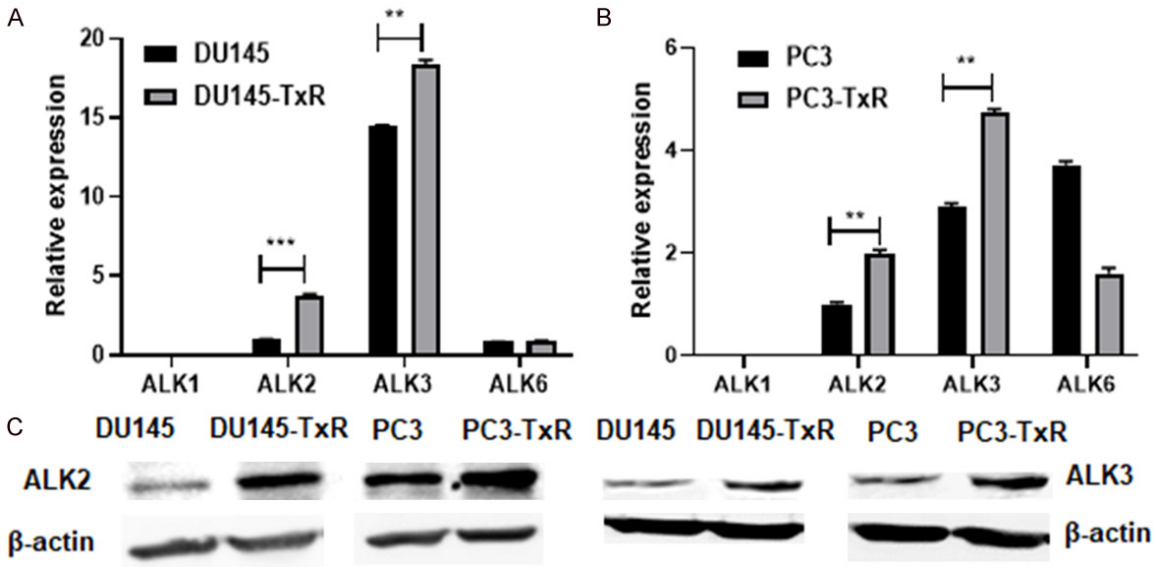

Figure 1. BMP type I receptors ALK2 and ALK3 expression is highly upregulated in chemoresistant prostate cancer cells. A and B. mRNA expression of all four BMP type I receptor members (ALK1, ALk2, ALK3 and ALK6) was examined by RT-PCT in both chemosensitive DU145 and PC3 cells and chemoresistant prostate cancer DU145-TxR and PC3-TxR cells (n=3, **P<0.01, ***P<0.001). C. Western blotting result confirmed that ALK2 and ALK3 expression levels were enhanced in DU145-TxR and PC3-TxR cells in comparison to DU145 and PC3 cells.

chemosensitive cell lines (DU145 and PC3) and the chemoresistant cell lines (DU145-TxR and PC3-TxR cells). The result indicates that ALK1 mRNA was not detectable in either the chemosensitive or the chemoresistant cells whereas mRNA expression levels of ALK2 and ALK3 were consistently increased in both chemoresistant DU145-TxR and PC3-TxR cells over the chemosensitive DU145 and PC3 cells (**Figure 1A** and **1B**). Interestingly, ALK6 mRNA expression remained unchanged in DU145 and DU145-TxR cells but was downregulated in the chemoresistant PC3-TxR cells in comparison to the PC3 cells.

To confirm the ALK2 and ALK3 expression at the protein level, we conducted Western Blotting. The result demonstrates that protein expressions of both ALK2 and ALK3 were dramatically enhanced in the chemoresistant DU145-TxR and PC3TxR cells in comparison to the chemosensitive DU145 and PC3 cells (**Figure 1C**).

In chemoresistant cells, the BMP signaling is highly activated which can be effectively blocked by DMH1

We next examined the BMP signaling in both the chemosensitive and the chemoresistant prostate cancer cells by Western Blotting. The result showed that phospho-Smad1/5/9 was barely detectable in the sensitive DU145 and PC3 cells but was strongly enhanced in the resistant DU145-TxR and PC3-TxR cells, indicating that the BMP signaling is highly activated in the chemoresistant prostate cancer cells (**Figure 2A**). Furthermore, we treated DU145-TxR and PC3-TxR cells with BMP signaling inhibitor DMH1 at 3 μM and 5 μM for overnight, and DMH1 effectively blocked the Smad1/5/9 phosphorylation in resistant DU145-TxR and PC3-TxR cells (**Figure 2A**). In consistence, the RT-PCR demonstrated that DMH1 dramatically down-regulated the mRNA expression of the BMP signaling target genes: Id1, Id2 and Id3 in DU145-TxR and PC3-TXR cells (**Figure 2B**). Taken together, those results indicate that the BMP signaling activation may be associated with the prostate cancer chemoresistance, and DMH1 effectively blocks the BMP signaling in the chemoresistant prostate cancer cells.

BMP signaling inhibition sensitizes the chemoresistant prostate cancer cells to docetaxel

Next, we examined the effects of BMP signaling inhibition by DMH1 on the sensitization of the chemoresistant prostate cancer cells to docetaxel. As expected, the resistant DU145-TxR and PC3-TxR cells were significantly resistant to docetaxel in contrast to the sensitive DU145 and PC3 cells, and DMH1 in combination with docetaxel didn't show any synergistic

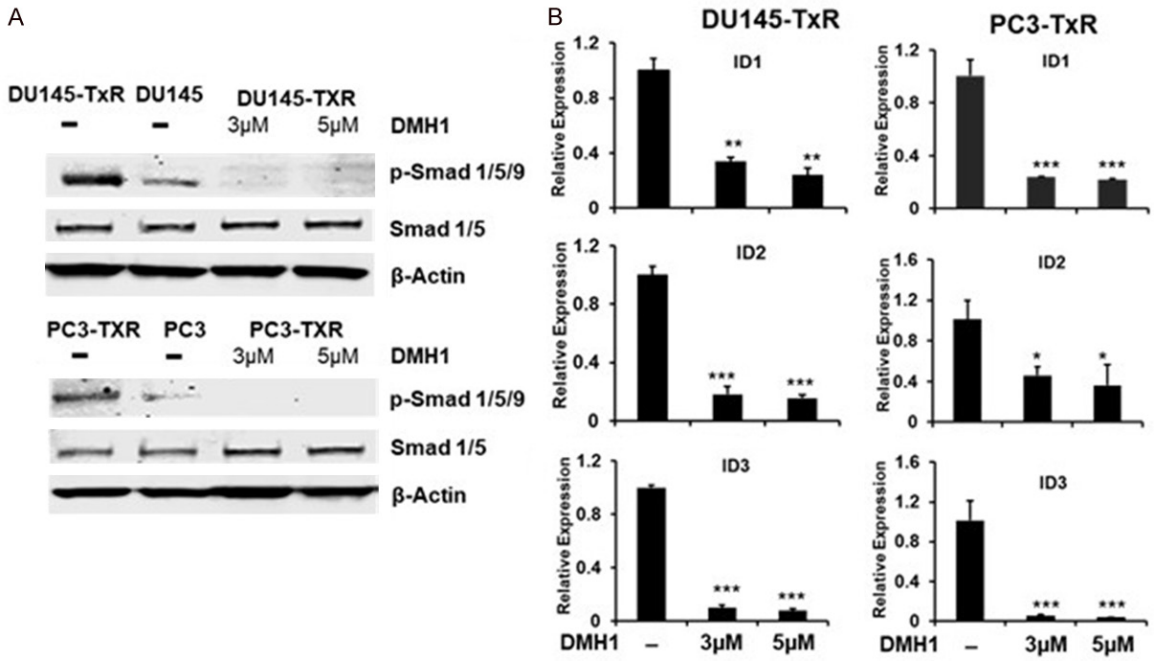

Figure 2. BMP signaling is activated in the chemoresistant prostate cancer cells and BMP inhibitor DMH1 effectively block BMP signaling. A. Western Blotting shows that phosph-Smad1/5/9, the essential intracellular effectors of BMP signaling, is highly up-regulated in DU145-TxR cells and PC3-TxR cells in contrast to that in DU145 or PC3 cells, and DMH1 treatment blocked phosph-Smad1/5/9. B. RT-PCR indicates that DMH1 effectively downregulated the mRNA expression of the BMP signaling target genes, Id1, Id2 and Id3. All data are compared to non-treatment group (n=3, *P<0.05, **P<0.01, ***P<0.001).

effect on the sensitive DU145 and PC3 cells versus docetaxel treatment alone (**Figure 3A** and **3B**). In contrast, DMH1 significantly sensitized the chemoresistant DU145-TxR and PC3-TxR cells to docetaxel in a dose-dependent manner, suggesting that the BMP signaling is associated with prostate cancer chemoresistance (**Figure 3C** and **3D**).

To verify that the sensitization effect of DMH1 on chemoresistant prostate cancer cells is through BMP signaling, we knocked down the BMP type I receptors ALK2 and ALK3 individually and simultaneously by siRNAs in DU145-TxR and PC3-TxR cells. As shown in **Figure 4A**, the sensitization of DU145-TxR and PC3-TxR cells to docetaxel was achieved by simultaneous knockdown of both ALK2 and ALK3, but not individual knockdown of either ALK2 or ALK3, suggesting that BMP signaling-mediated by either ALK2 or ALK3 is implicated in prostate cancer chemoresistance. In addition, the RT-PCR result confirms that ALK2 and ALK3 were effectively knocked down in the DU145-TxR and PC3-TxR cells (**Figure 4B**).

DMH1 decreases the migration and invasion of the chemoresistant prostate cancer cells

Since active migration and invasion are important for the progression of cancer cells, we performed *in-vitro* cell migration and invasion assays in the chemoresistant prostate cancer cells. The scratch-wound assay was conducted to determine cell migration by creating wound gaps in the cultured DU145-TxR and PC3-TxR cells. The cells were treated with DMSO, 1 nM docetaxel, 3 μM DMH1, and 1 nM docetaxel combined with 3 μM DMH1 for 24 hrs respectively, and the gap distances were then normalized with the initially measured distances. The result showed that 1 nM docetaxel did not significantly change the cell migration in both DU145-TxR and PC3-TXR cells where 3 μM DMH1 alone statistically significantly slowed down the migration by 26.7% for DU145-TxR cells and 30.2% for PC3-TxT cells compared to the DMSO control (**Figure 5A**). The docetaxel combined with DMH1 treatment slowed down the migration by approximately 89% in both DU145-TxR cells and PC3-TXR cells in comparison to the DMSO controls.

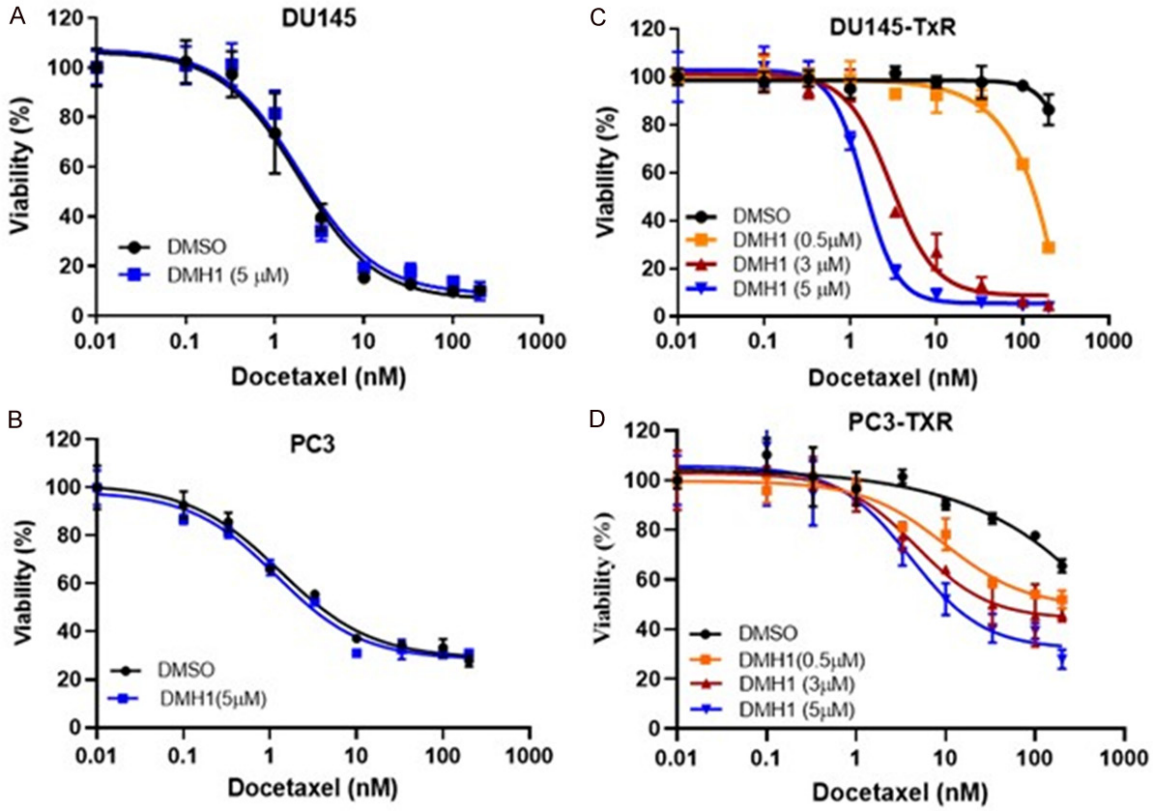

Figure 3. BMP signaling inhibitor DMH1 sensitizes chemoresistant DU145-TxR and PC3-TxR cells to docetaxel in dose-dependent manners. DMH1 has no effects on the sensitivity of DU145 and PC3 cells to docetaxel (A and B), but it dramatically sensitizes the resistant DU145-TxR and PC3-TxR cells to docetaxel in dose-dependent manners (C and D). The nonlinear regression was used to generate curves in the Prism software. Note: The X-axis is in logarithmic scale. The cells were treated with vehicle DMSO, or DMH1 (0.5 μM, 3 μM and 5 μM) with combination of docetaxel (0, 0.1, 0.33, 1, 3.3, 10, 33.3, 100 and 200 nM) for 72 h. The control cell viability (no docetaxel) was designated as 100%, and the cell viabilities were normalized to the control cell viability without docetaxel treatment.

The cell invasion was measured by using a modified Boyden chamber assay. Both DU145-TxR cells and PC3-TxR cells were seeded on Matrigel-coated chambers, followed by 72 hr-incubation with DMSO, 1 nM docetaxel, 3 μM DMH1, and 1 nM docetaxel combined with 3 μM DMH1, respectively. DMH1 treatment alone dramatically reduced the cell invasion of DU145-TxR cells and PC3-TxR cells through Matrigel-coated membranes by approximately 47.6% and 68.5%, respectively, in comparison to the control (**Figure 5B**). In addition, treatment with the combination of docetaxel and DMH1 decreased the cell invasion by 89.6% in DU145-TxR cells and 89.1% in PC3-TxR cells (**Figure 5B**). In summary, DMH1 alone or combined with docetaxel dramatically decreased the migration and invasion of the chemoresistant prostate cancer cells.

DMH1 attenuates chemoresistant prostate tumor growth in the mouse xenograft model

We next assessed the effect of DMH1 on chemoresistant prostate cancer growth in a mouse xenograft model. One week after tumor implantation, the animals with growing tumors of proper sizes were divided into four groups treated by vehicle, docetaxel, DMH1, and docetaxel combined with DMH1 (n=9 for each group) respectively. The duration of the treatment was 16 days from the time of the first drug injection. The result showed that the average tumor volume in the docetaxel treatment group was slightly smaller (but not statistically significant) than that in the vehicle control group (**Figure 6A**). Whereas the average tumor volumes in the DMH1 treatment group and docetaxel combined with DMH1 group were significantly decreased on days 14, 18, 21 and 23 after

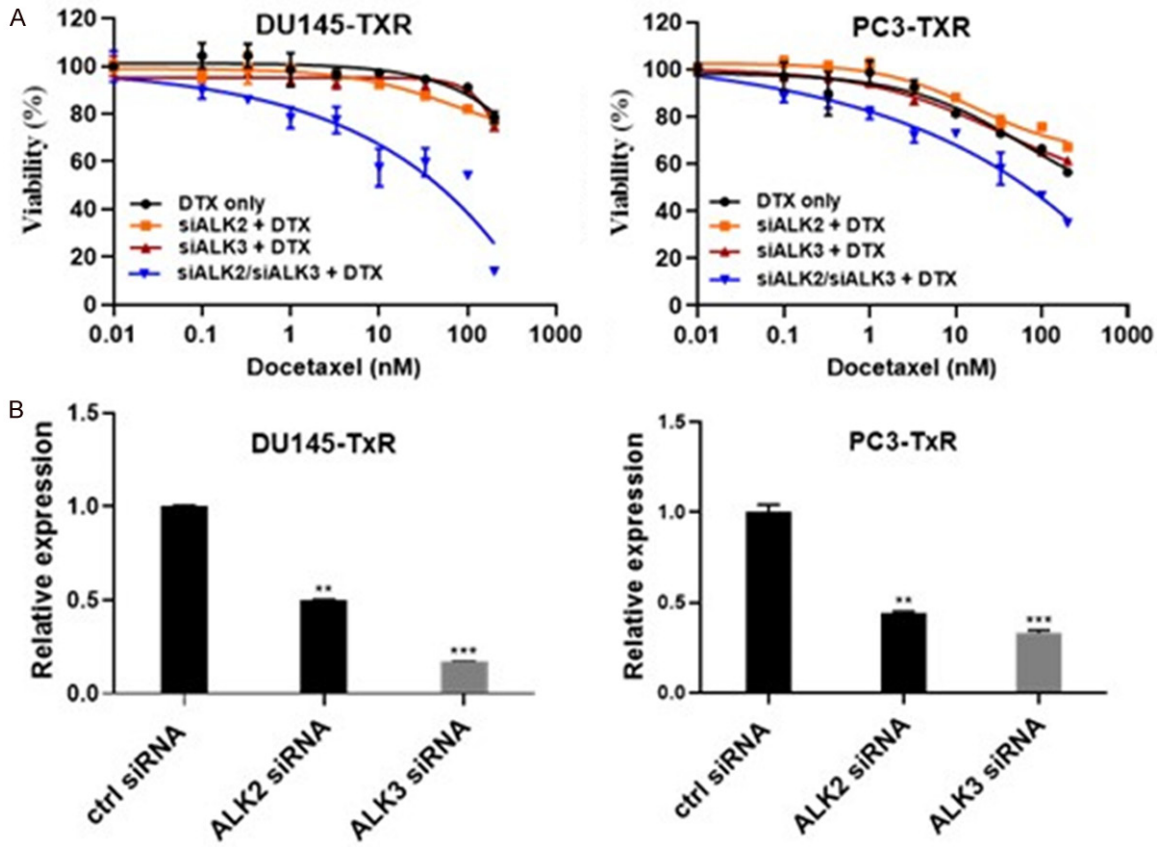

Figure 4. Knockdown of both ALK2 and ALK3 by siRNAs significantly sensitizes the chemoresistant DU145-TxR and PC3-TxR cells to docetaxel. A. siRNA knockdown of ALK2, ALK3 simultaneously sensitized the DU145-TxR and PC3-TxR cells to docetaxel (DTX in Figure). B. RT-PCR confirmed that siRNAs significantly knocked down both ALK2 and ALK3 simultaneously in DU145-TxR and PC3-TxR cells. All data are compared to control group (n=3, **P<0.01, ***P<0.001).

tumor implantation and decreased by 34.8% and 57.6% in comparison to the vehicle control group on day 23, respectively (**Figure 6A**). In addition, the body weight losses of the mice in all four groups were below the generally accepted body-weight reduction (20% or more) [14] (data not shown).

To further examine the effect of DMH1 on tumor cell proliferation *in vivo*, the fixed tumor tissue samples from each group were sliced and subjected to immunostaining with human specific proliferation marker Ki-67. The confocal images showed apparent decreases of Ki67 positive cells in the DMH1 group and DMH1/Docetaxel group versus the vehicle group, with a most significant decrease of Ki-67 positive cells in the DMH1/Docetaxel group (**Figure 6B**). The quantified data shows that human-specific Ki-67 positive cells in the DMH1 group and the DMH1/Docetaxel group were decreased by 46.6% and 54.2%, respectively. In conclusion, the mouse xenograft study indicates that DMH1 alone and in combination with docetaxel dramatically attenuated chemoresistant prostate cancer cell proliferation *in vivo*.

DMH1 attenuates stem-like properties of chemoresistant prostate cancer cells

The CSCs are thought to be essential for cancer initiation, metastasis, and chemoresistance [15-17]. Therefore, we examined the effects of DMH1 on the CSCs by the sphere-formation assay, a method used for studying the CSCs' stemness [18]. In brief, the chemoresistant DU-145-TxR and PC3-TxR cells were plated on a low-attached 6-well-plate for the suspension culture for 14 days, and the sphere-forming capacity was assessed by the number of colonies in size larger than 50 μm diameter. The result shows that docetaxel treat-

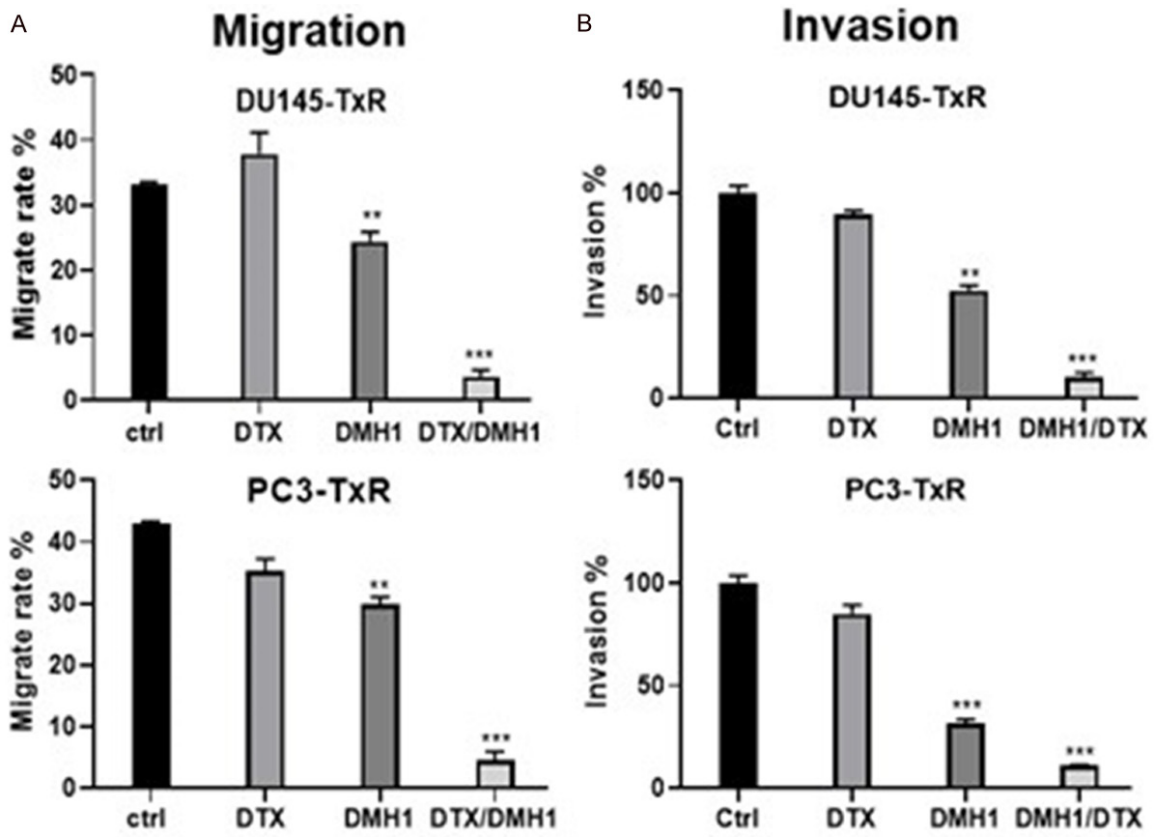

Figure 5. DMH1 decreases migration and invasion of chemoresistant prostate cancer cells. A. Effects of DMH1 (3 μM), Docetaxel (DTX, 1 nM) and their combination (DMH1/DTX) on migration of the chemoresistant prostate cancer DU145-TxR and PC3-TxR cells were determined using the Cell Scratch-Wound Assay after 24-hour treatment. Cell migrations were quantified by the gap distances after 22-hr treatment normalized with the initial gap distances (n=3, **P<0.01, ***P<0.001). B. Effects of DMH1 (3 μM), Docetaxel (DTX, 1 nM) and their combination (DMH1/DTX) on invasion of DU145-TxR and PC3-TxR cells were determined using modified Boyden chamber assay in a 24-Multiwell Insert System (8 μM membrane, BD Biosciences) coated with Matrigel. The cells were treated for 72 hours, and the invading cell percentages were normalized to the DMSO vehicle treated controls. All data are compared to control group (n=3, **P<0.01, ***P<0.001).

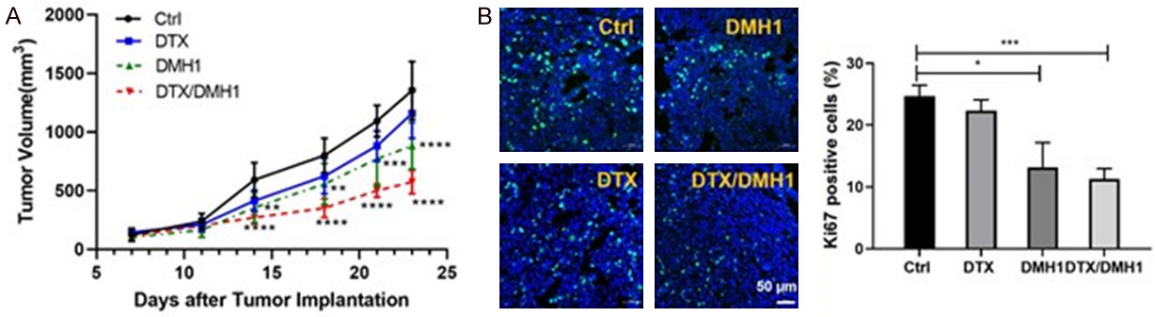

Figure 6. DMH1 in combination with Docetaxel decreases chemoresistant prostate tumor growth in the mouse xenograft model. A. The PC3-TxR cells were implanted into dorsal flank region of the NSG male mice. Seven days after tumor implantation, the animals will be divided into four groups with nine mice in each group: the vehicle (12.5% HP-β-CD) group, docetaxel (DTX, 20 mg/kg solution) group, DMH1 (5 mg/kg protonated DMH1 chloride dissolved in 12.5% HP-β-CD) group and docetaxel plus DMH1 (20 mg/kg solution DTX and 5 mg/kg protonated DMH1 chloride dissolved in 12.5% HP-β-CD) treatment group. Vehicle or DMH1 was intraperitoneally (i.p.) injected every other day to the mice while docetaxel was intravenously (i.v.) injected once per week for twice. The data was expressed as mean ± standard deviation. B. Representative tumor tissues were stained for human specific Ki67 proliferation marker and nucleus marker DAPI. All data are compared to the control group (*P<0.05, **P<0.01, ***P<0.001, ****P<0.0001).

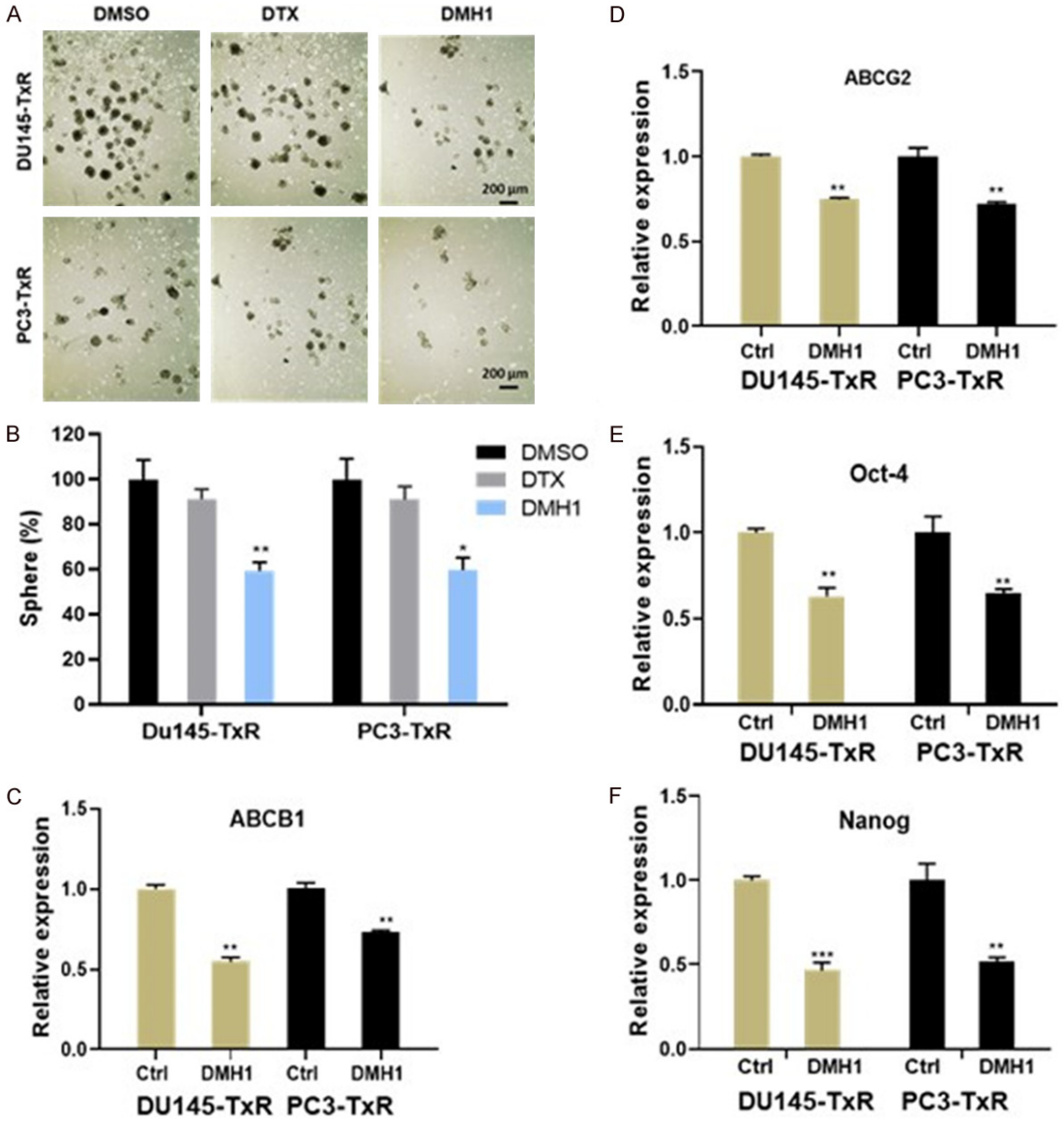

Figure 7. DMH1 inhibits sphere formation and attenuates the expression of CSCs' markers in chemoresistant prostate cancer cells. A. Representative images for the sphere formation assay in chemoresistant DU145-TxR and PC3-TxR cells treated with vehicle DMSO, 1 nM Docetaxel (DTX) and 3 μM DMH1. B. Quantification of spheres treated by DMSO, 1 nM Docetaxel (DTX) and 3 μM DMH1 (*P<0.05, **P<0.01). C-F. mRNA expression levels of ABCB1, ABCG2, OCT-4 and Nanog are statistically significantly down-regulated in resistant DU145-TxR and PC3-TxR cells treated with 3 μM DMH1 (**P<0.01, ***P<0.001).

ment did not statistically significantly alter the sphere number in DU145-TxR and PC3-TxR cells. In contrast, 3 μM DMH1 treatment led to 40.6% and 40.3% of decreases in the sphere numbers of DU145-TxR and of PC3-TxR cells, respectively (**Figure 7A** and **7B**). Furthermore, we examined whether DMH1 alters the expression of CSCs' markers in the DU-145-TxR and PC3-TxR cells. ABCB1, and ABCG2, Oct-4 and Nanog are marker genes known for prostate CSC [19-25], and the RT-PCR result demonstrated that DMH1 could dramatically down-regulate the expression of all the four stem cell marker genes in DU-145-TXR and PC3-TxR cells (**Figure 7C-F**). In addition, Western blotting study indicates that DMH1 inhibits CSCs'

marker ABCG2 expression in chemoresistant prostate cancer cells (Supplementary Figure 1). In summary, DMH1 treatment disrupted the CSCs' stemness in the chemoresistant prostate cancer cells.

Discussion and conclusion

Cumulative studies have shown that altered BMP signaling is implicated in multiple types of cancer including hepatocellular carcinoma, colorectal cancer, lung cancer, breast cancer and prostate cancer [7, 12, 13, 26-31]. However, few studies on the role of the BMP signaling in the cancer chemoresistance have been reported. We found that the expressions of ALK2 and ALK3 were enhanced and the BMP signaling was highly activated in the chemoresistant prostate cancer cells in comparison to the chemosensitive prostate cancer cells, suggesting that BMP signaling activation may be associated with prostate cancer chemoresistance. This is consistent with the fact that BMP inhibitor DMH1 or knockdown of both ALK2 and ALK3 receptors dramatically sensitized the chemoresistant prostate cancer cells to docetaxel. In addition, DMH1 alone or in combination with docetaxel effectively decreased the migration and invasion of the chemoresistant prostate cancer cells *in vitro*, and significantly attenuated tumor growth in the immunodeficient NSG mice implanted with the chemoresistant PC3-TxR cells *in vivo*, suggesting that BMP inhibition by DMH1 could overcome the chemoresistance of prostate cancer to docetaxel. In consistence, the association of the BMP signaling activation with the cancer chemoresistance is supported by some reports. For instance, in ovarian cancer, human carcinoma-associated mesenchymal stem cells activate the BMP and Hedgehog signaling pathways which increase the proliferation of CSCs and enhance the chemoresistance of ovarian cancer [32]. In addition, a very recent report showed that BMP signaling activated by BMP4 increases the chemoresistance of breast cancer cells [33].

BMP signaling is known to regulate the CSCs' self-renewal and the CSCs' stemness is accountable for the cancer chemoresistance [15, 17, 34-36]. For instance, the hyperactivation of BMP signaling promotes CSCs' proliferation in breast cancer and oral squamous cell carcinoma [37, 38]. In consistence, our study has demonstrated that DMH1 dramatically inhibited the sphere formation and down-regulated the expression levels of CSCs' markers ABCB1, ABCG2, OCT-4 and Nanog in the chemoresistant prostate cancer cells, suggesting that DMH1 attenuated the CSCs' stemness in chemoresistant prostate cancer.

One limitation of this study is that no prostate tissue samples from human patients with chemoresistant prostate cancer have been investigated, and it remains to be verified whether our findings of BMP signaling in the docetaxel-resistant cell lines faithfully recapitulate characteristics of human prostate tissues of the docetaxel-treated prostate cancer patients. Nevertheless, the taxoid (docetaxel or paclitaxel)-resistant cancer cell lines have been widely accepted as reliable and alternative *in-vitro* models to study chemo-resistance in many types of cancer including ovarian cancer, breast cancer, lung cancer and prostate cancer [15, 39-53]. Moreover, Domingo et al has confirmed that the docetaxel-resistant prostate cancer cell lines used in our study display phenotypes similar to human prostate tissues of the docetaxel-treated prostate cancer patients, supporting docetaxel-resistant prostate cancer cell lines as a reliable model for the prostate cancer chemo-resistance [54].

In summary, our study indicates that the BMP signaling is associated with the prostate cancer chemoresistance and targeting BMP signaling with selective type I receptor inhibitors, like DMH1, may represent a novel therapeutic strategy to overcome the chemoresistance of prostate cancer.

Acknowledgements

This research was funded by Elsa U Pardee Foundation to J.H.

Disclosure of conflict of interest

None.

Address correspondence to: Jijun Hao, College of Veterinary Medicine, Western University of Health Sciences, 309 E 2nd Street, Pomona, CA 91766, USA. Tel: 909-469-8686; Fax: 909-469-5635; E-mail: jhao@westernu.edu

References

[1] Sung H, Ferlay J, Siegel RL, Laversanne M, Soerjomataram I, Jemal A and Bray F. Global can-

cer statistics 2020: GLOBOCAN estimates of incidence and mortality worldwide for 36 cancers in 185 countries. CA Cancer J Clin 2021; 71: 209-249.
[2] Bishr M and Saad F. Overview of the latest treatments for castration-resistant prostate cancer. Nat Rev Urol 2013; 10: 522-528.
[3] Huggins C. The hormone-dependent cancers. JAMA 1963; 186: 481-483.
[4] Huggins C and Hodges CV. Studies on prostatic cancer. I. The effect of castration, of estrogen and of androgen injection on serum phosphatases in metastatic carcinoma of the prostate. J Urol 2002; 168: 9-12.
[5] Tannock IF, de Wit R, Berry WR, Horti J, Pluzanska A, Chi KN, Oudard S, Theodore C, James ND, Turesson I, Rosenthal MA and Eisenberger MA; TAX 327 Investigators. Docetaxel plus prednisone or mitoxantrone plus prednisone for advanced prostate cancer. N Engl J Med 2004; 351: 1502-1512.
[6] Miyazono K, Maeda S and Imamura T. BMP receptor signaling: transcriptional targets, regulation of signals, and signaling cross-talk. Cytokine Growth Factor Rev 2005; 16: 251-263.
[7] Kim IY, Lee DH, Ahn HJ, Tokunaga H, Song W, Devereaux LM, Jin D, Sampath TK and Morton RA. Expression of bone morphogenetic protein receptors type-IA, -IB and -II correlates with tumor grade in human prostate cancer tissues. Cancer Res 2000; 60: 2840-2844.
[8] Kim IY, Lee DH, Lee DK, Ahn HJ, Kim MM, Kim SJ and Morton RA. Loss of expression of bone morphogenetic protein receptor type II in human prostate cancer cells. Oncogene 2004; 23: 7651-7659.
[9] Ye L, Lewis-Russell JM, Kyanaston HG and Jiang WG. Bone morphogenetic proteins and their receptor signaling in prostate cancer. Histol Histopathol 2007; 22: 1129-1147.
[10] Hamdy FC, Autzen P, Robinson MC, Horne CH, Neal DE and Robson CN. Immunolocalization and messenger RNA expression of bone morphogenetic protein-6 in human benign and malignant prostatic tissue. Cancer Res 1997; 57: 4427-4431.
[11] Harris SE, Harris MA, Mahy P, Wozney J, Feng JQ and Mundy GR. Expression of bone morphogenetic protein messenger RNAs by normal rat and human prostate and prostate cancer cells. Prostate 1994; 24: 204-211.
[12] Horvath LG, Henshall SM, Kench JG, Turner JJ, Golovsky D, Brenner PC, O'Neill GF, Kooner R, Stricker PD, Grygiel JJ and Sutherland RL. Loss of BMP2, Smad8, and Smad4 expression in prostate cancer progression. Prostate 2004; 59: 234-242.
[13] Hao J, Lee R, Chang A, Fan J, Labib C, Parsa C, Orlando R, Andresen B and Huang Y. DMH1, a small molecule inhibitor of BMP type i receptors, suppresses growth and invasion of lung cancer. PLoS One 2014; 9: e90748.
[14] Talbot SR, Biernot S, Bleich A, van Dijk RM, Ernst L, Hager C, Helgers SOA, Koegel B, Koska I, Kuhla A, Miljanovic N, Muller-Graff FT, Schwabe K, Tolba R, Vollmar B, Weegh N, Wolk T, Wolf F, Wree A, Zieglowski L, Potschka H and Zechner D. Defining body-weight reduction as a humane endpoint: a critical appraisal. Lab Anim 2020; 54: 99-110.
[15] Ni J, Cozzi P, Hao J, Duan W, Graham P, Kearsley J and Li Y. Cancer stem cells in prostate cancer chemoresistance. Curr Cancer Drug Targets 2014; 14: 225-240.
[16] Yun EJ, Lo UG and Hsieh JT. The evolving landscape of prostate cancer stem cell: therapeutic implications and future challenges. Asian J Urol 2016; 3: 203-210.
[17] Vidal SJ, Rodriguez-Bravo V, Galsky M, Cordon-Cardo C and Domingo-Domenech J. Targeting cancer stem cells to suppress acquired chemotherapy resistance. Oncogene 2014; 33: 4451-4463.
[18] Bahmad HF, Cheaito K, Chalhoub RM, Hadadeh O, Monzer A, Ballout F, El-Hajj A, Mukherji D, Liu YN, Daoud G and Abou-Kheir W. Sphere-formation assay: three-dimensional in vitro culturing of prostate cancer stem/progenitor sphere-forming cells. Front Oncol 2018; 8: 347.
[19] Sabnis NG, Miller A, Titus MA and Huss WJ. The efflux transporter ABCG2 maintains prostate stem cells. Mol Cancer Res 2017; 15: 128-140.
[20] Badic B, Durand S, El Khoury F, De La Grange P, Gentien D, Simon B, Le Jossic-Corcos C and Corcos L. Prognostic impact of cancer stem cell markers ABCB1, NEO1 and HIST1H2AE in colorectal cancer. Am J Transl Res 2020; 12: 5797-5807.
[21] Guzel E, Karatas OF, Duz MB, Solak M, Ittmann M and Ozen M. Differential expression of stem cell markers and ABCG2 in recurrent prostate cancer. Prostate 2014; 74: 1498-1505.
[22] Jiang Y, He Y, Li H, Li HN, Zhang L, Hu W, Sun YM, Chen FL and Jin XM. Expressions of putative cancer stem cell markers ABCB1, ABCG2, and CD133 are correlated with the degree of differentiation of gastric cancer. Gastric Cancer 2012; 15: 440-450.
[23] Rasti A, Mehrazma M, Madjd Z, Abolhasani M, Saeednejad Zanjani L and Asgari M. Co-expression of cancer stem cell markers OCT4 and NANOG predicts poor prognosis in renal cell carcinomas. Sci Rep 2018; 8: 11739.
[24] Mohiuddin IS, Wei SJ and Kang MH. Role of OCT4 in cancer stem-like cells and chemother-

apy resistance. Biochim Biophys Acta Mol Basis Dis 2020; 1866: 165432.
[25] Vasefifar P, Motafakkerazad R, Maleki LA, Najafi S, Ghrobaninezhad F, Najafzadeh B, Alemohammad H, Amini M, Baghbanzadeh A and Baradaran B. Nanog, as a key cancer stem cell marker in tumor progression. Gene 2022; 827: 146448.
[26] Li Q, Gu X, Weng H, Ghafoory S, Liu Y, Feng T, Dzieran J, Li L, Ilkavets I, Kruithof-de Julio M, Munker S, Marx A, Piiper A, Augusto Alonso E, Gretz N, Gao C, Wolfl S, Dooley S and Breitkopf-Heinlein K. Bone morphogenetic protein-9 induces epithelial to mesenchymal transition in hepatocellular carcinoma cells. Cancer Sci 2013; 104: 398-408.
[27] Deng G, Zeng S, Qu Y, Luo Q, Guo C, Yin L, Han Y, Li Y, Cai C, Fu Y and Shen H. BMP4 promotes hepatocellular carcinoma proliferation by autophagy activation through JNK1-mediated Bcl-2 phosphorylation. J Exp Clin Cancer Res 2018; 37: 156.
[28] Lorente-Trigos A, Varnat F, Melotti A and Ruiz i Altaba A. BMP signaling promotes the growth of primary human colon carcinomas in vivo. J Mol Cell Biol 2010; 2: 318-332.
[29] Yokoyama Y, Watanabe T, Tamura Y, Hashizume Y, Miyazono K and Ehata S. Autocrine BMP-4 signaling is a therapeutic target in colorectal cancer. Cancer Res 2017; 77: 4026-4038.
[30] Bach DH, Park HJ and Lee SK. The dual role of bone morphogenetic proteins in cancer. Mol Ther Oncolytics 2017; 8: 1-13.
[31] Owens P, Pickup MW, Novitskiy SV, Giltnane JM, Gorska AE, Hopkins CR, Hong CC and Moses HL. Inhibition of BMP signaling suppresses metastasis in mammary cancer. Oncogene 2015; 34: 2437-2449.
[32] Coffman LG, Choi YJ, McLean K, Allen BL, di Magliano MP and Buckanovich RJ. Human carcinoma-associated mesenchymal stem cells promote ovarian cancer chemotherapy resistance via a BMP4/HH signaling loop. Oncotarget 2016; 7: 6916-6932.
[33] Sharma R, Gogoi G, Saikia S, Sharma A, Kalita DJ, Sarma A, Limaye AM, Gaur MK, Bhattacharyya J and Jaganathan BG. BMP4 enhances anoikis resistance and chemoresistance of breast cancer cells through canonical BMP signaling. J Cell Commun Signal 2022; 16: 191-205.
[34] Galletti G, Leach BI, Lam L and Tagawa ST. Mechanisms of resistance to systemic therapy in metastatic castration-resistant prostate cancer. Cancer Treat Rev 2017; 57: 16-27.
[35] Seruga B, Ocana A and Tannock IF. Drug resistance in metastatic castration-resistant prostate cancer. Nat Rev Clin Oncol 2011; 8: 12-23.
[36] Baccelli I and Trumpp A. The evolving concept of cancer and metastasis stem cells. J Cell Biol 2012; 198: 281-293.
[37] Balboni AL, Hutchinson JA, DeCastro AJ, Cherukuri P, Liby K, Sporn MB, Schwartz GN, Wells WA, Sempere LF, Yu PB and DiRenzo J. ΔNp63α-mediated activation of bone morphogenetic protein signaling governs stem cell activity and plasticity in normal and malignant mammary epithelial cells. Cancer Res 2013; 73: 1020-1030.
[38] Qiao B, Johnson NW, Chen X, Li R, Tao Q and Gao J. Disclosure of a stem cell phenotype in an oral squamous cell carcinoma cell line induced by BMP-4 via an epithelial-mesenchymal transition. Oncol Rep 2011; 26: 455-461.
[39] Duan Z, Lamendola DE, Duan Y, Yusuf RZ and Seiden MV. Description of paclitaxel resistance-associated genes in ovarian and breast cancer cell lines. Cancer Chemother Pharmacol 2005; 55: 277-285.
[40] Sun NK, Huang SL, Chang PY, Lu HP and Chao CC. Transcriptomic profiling of taxol-resistant ovarian cancer cells identifies FKBP5 and the androgen receptor as critical markers of chemotherapeutic response. Oncotarget 2014; 5: 11939-11956.
[41] Wang NN, Zhao LJ, Wu LN, He MF, Qu JW, Zhao YB, Zhao WZ, Li JS and Wang JH. Mechanistic analysis of taxol-induced multidrug resistance in an ovarian cancer cell line. Asian Pac J Cancer Prev 2013; 14: 4983-4988.
[42] Ajabnoor GM, Crook T and Coley HM. Paclitaxel resistance is associated with switch from apoptotic to autophagic cell death in MCF-7 breast cancer cells. Cell Death Dis 2012; 3: e260.
[43] Chen SY, Hu SS, Dong Q, Cai JX, Zhang WP, Sun JY, Wang TT, Xie J, He HR, Xing JF, Lu J and Dong YL. Establishment of paclitaxel-resistant breast cancer cell line and nude mice models, and underlying multidrug resistance mechanisms in vitro and in vivo. Asian Pac J Cancer Prev 2013; 14: 6135-6140.
[44] Chu JJ, Chiang CD, Rao CS, Chang WM and Lai YK. Establishment and characterization of a paclitaxel-resistant human non-small cell lung cancer cell line. Anticancer Res 2000; 20: 2449-2456.
[45] Goncalves A, Braguer D, Kamath K, Martello L, Briand C, Horwitz S, Wilson L and Jordan MA. Resistance to taxol in lung cancer cells associated with increased microtubule dynamics. Proc Natl Acad Sci U S A 2001; 98: 11737-11742.
[46] Kim JJ, Yin B, Christudass CS, Terada N, Rajagopalan K, Fabry B, Lee DY, Shiraishi T, Getzen-

berg RH, Veltri RW, An SS and Mooney SM. Acquisition of paclitaxel resistance is associated with a more aggressive and invasive phenotype in prostate cancer. J Cell Biochem 2013; 114: 1286-1293.

[47] Liu Z, Zhu G, Getzenberg RH and Veltri RW. The upregulation of PI3K/Akt and MAP kinase pathways is associated with resistance of microtubule-targeting drugs in prostate cancer. J Cell Biochem 2015; 116: 1341-1349.

[48] Singh S, Chitkara D, Mehrazin R, Behrman SW, Wake RW and Mahato RI. Chemoresistance in prostate cancer cells is regulated by miRNAs and hedgehog pathway. PLoS One 2012; 7: e40021.

[49] Takeda M, Mizokami A, Mamiya K, Li YQ, Zhang J, Keller ET and Namiki M. The establishment of two paclitaxel-resistant prostate cancer cell lines and the mechanisms of paclitaxel resistance with two cell lines. Prostate 2007; 67: 955-967.

[50] Teraishi F, Wu S, Sasaki J, Zhang L, Zhu HB, Davis JJ and Fang B. P-glycoprotein-independent apoptosis induction by a novel synthetic compound, MMPT [5-[(4-methylphenyl)methylene]-2-(phenylamino)-4(5H)-thiazolone]. J Pharmacol Exp Ther 2005; 314: 355-362.

[51] Zuo KQ, Zhang XP, Zou J, Li D and Lv ZW. Establishment of a paclitaxel resistant human breast cancer cell strain (MCF-7/Taxol) and intracellular paclitaxel binding protein analysis. J Int Med Res 2010; 38: 1428-1435.

[52] Li Y, Zeng Y, Mooney SM, Yin B, Mizokami A, Namiki M and Getzenberg RH. Resistance to paclitaxel increases the sensitivity to other microenvironmental stresses in prostate cancer cells. J Cell Biochem 2011; 112: 2125-2137.

[53] von Boehmer L, Keller L, Mortezavi A, Provenzano M, Sais G, Hermanns T, Sulser T, Jungbluth AA, Old LJ, Kristiansen G, van den Broek M, Moch H, Knuth A and Wild PJ. MAGE-C2/CT10 protein expression is an independent predictor of recurrence in prostate cancer. PLoS One 2011; 6: e21366.

[54] Domingo-Domenech J, Vidal SJ, Rodriguez-Bravo V, Castillo-Martin M, Quinn SA, Rodriguez-Barrueco R, Bonal DM, Charytonowicz E, Gladoun N, de la Iglesia-Vicente J, Petrylak DP, Benson MC, Silva JM and Cordon-Cardo C. Suppression of acquired docetaxel resistance in prostate cancer through depletion of notch- and hedgehog-dependent tumor-initiating cells. Cancer Cell 2012; 22: 373-388.

Supplementary Table 1. The primer sets used in the study

Genes	Oligonucleotides
Human GAPDH	5'-GGTGTGAACCATGAGAAGTATGA-3' (forward)
	5'-GTCCTTCCACGATACCAAAG-3' (reverse)
Human ALK1	5'-CAACAGTCCAGAGAAGCCTAAA-3' (forward)
	5'-CTCACACTACCTCTACCCAGATA-3' (reverse)
Human ALK2	5'-GTGACCAAGAGCCTGCATTA-3' (forward)
	5'-TTGGGCTTCTCATCTTCCATAC-3' (reverse)
Human ALK3	5'-AGTGGGTCTGGACTACCTTTA-3' (forward)
	5'-GCCCATCCATACTTCTCCATATC-3' (reverse)
Human ALK6	5'-CCTATACACCACAGGGCTTTAC-3' (forward)
	5'-CGAGGTCTGGTTTCTTGTCTT-3' (reverse)
Human ABCG2	5'-GTGTGTCTGGAGGAGAAAGAAA-3' (forward)
	5'-GCTTGAGTCTAAGCCAGTTGTA-3' (reverse)
Human ABCB1	5'-TGCTGGTTGCTGCTTACA-3' (forward)
	5'-GCCTATCTCCTGTCGCATTATAG-3' (reverse)
Human Id1	5'-GCTGTTACTCACGCCTCAA-3' (forward)
	5'-CAACTGAAGGTCCCTGATGTAG-3' (reverse)
Human Id2	5'-GCACGTCATCGACTACATCTT-3' (forward)
	5'-AGGATGCTGATATCCGTGTTG-3' (reverse)
Human Id3	5'-CGACATGAACCACTGCTACTC-3' (forward)
	5'-GATGACGCGCTGTAGGATTT-3' (reverse)
Human OCT4	5'-GAGAGGCAACCTGGAGAATTT-3' (forward)
	5'-ACTCGGACCACATCCTTCT-3' (reverse)
Human Nanog	5'-ACCCAATCCTGGAACAATCAG-3' (forward)
	5'-AGTCACTGGCAGGAGAATTTG-3' (reverse)

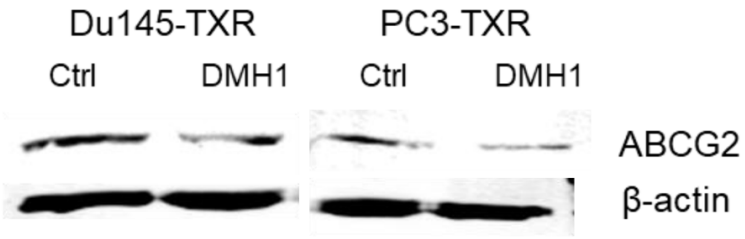

Supplementary Figure 1. Western blotting study indicates that DMH1 inhibits CSCs' marker ABCG2 expression in chemoresistant prostate cancer cells.